Metamaterial Sensor for Transformer Oil, and Microfluidics

Mehmet Bakır [1], Muharrem Karaaslan [2], Faruk Karadag [3], Sekip Dalgac [2], Emin Ünal [2], and Oğuzhan Akgöl [2]

[1] Department of Computer Engineering
Bozok University, Yozgat, 66200, Turkey
mehmet.bakir@bozok.edu.tr

[2] Iskenderun Technical University
Department of Electrical and Electronics Engineering, Hatay, 31200, Turkey
Muharrem.karaaslan@iste.edu.tr, emin.unal@iste.edu.tr, oguzhan.akgol@iste.edu.tr

[3] Department of Physics
Cukurova University, Adana, 01030, Turkey
fkaradag.cu.edu.tr

Abstract **─** Metamaterial sensor which is composed of split square rings to operate in X band for liquid and microfluidics has been proposed in this study. For measurement and simulation, we have designed and manufactured a sample holder for easy injection and measurement of fluids. Dielectric properties of the fluid samples have been changed according to the usage time, humidity etc. Proposed structure reacts to the dielectric constants of the transformer oil or the other microfluidics by resonance frequency which is also validated by simulation and testing. While 70MHz bandwidth change in the resonance frequency for transformer oil has been observed, it dramatically increases to 210MHz and decreases to 40MHz for methanol and olive oil adulteration. Reflection coefficient measurements for clear (unused) transformer oil, methanol and olive oil along with corn oil have been performed. Tested results are generally compatible with the simulated ones. Proposed structure, can be effectively used for liquids whose dielectric constant varying from 2 to 24. Simulation study shows us that the proposed structure gives 560MHz bandwidth when clear transformer oil is replaced with acetone. Implementation of transformer oil as well as microfluidics with high quality factor is the novel side of proposed sensor study.

Index Terms **─** Industrial oil, olive oil, metamaterials, microfluidics, sensor.

I. INTRODUCTION

Permittivity of a material gives us lots of information about purity, temperature and humidity since it changes according to these environmental factors and purity. This information can easily be used for developing sensors in microwave frequencies [1-5]. For this purpose, different techniques such as resonance cavity [6], resonant/reflection or transmission [7-8] can be employed. Metamaterials which are manmade structures showing exotic properties like negative refractive index have effectively been used in antennas, cloaking, microwave absorbers, energy harvesting and sensor applications [9-15].

Sensor applications of metamaterials can be realized by taking split ring resonators (SRR) as the basis for concentrating the electromagnetic field and sensing related parameters according to the materials' complex permittivity changes. There are some studies in the literature investigating the use of metamaterials as liquid sensors. In [16], spiral shaped MTM coupled with microfluidic channel is experimentally realized and the corresponding resonance frequency shifts 150MHz according to dielectric constant changes from 25 to 75. In [17], a microwave microfluidic sensor is proposed to determine the dielectric properties of alcohol derivatives including methanol, ethanol and hexane and a maximum of 61.5MHz bandwidth is observed. In [18], a microfluidic sensor is implemented from a single SRR for purity sensing of methanol and ethanol mixtures with water. Experimental study results showed 90MHz bandwidth with a Q factor of 28. In [19], a complementary SRR type MTM is proposed and 300MHz bandwidth is obtained with considerably small Q factors. In [20], three different types of sensor applications demonstrated experimentally and numerically by utilization of microfluidic channel. In that study 200MHz bandwidth with high Q factor has been obtained.

Most MTM sensors employ the changes in resonance frequency which shifts according to the parameter which

Submitted On: July 19, 2018
Accepted On: December 25, 2018

is being sensed [21-22]. In addition to the microfluidic sensor applications, fuel adulteration and transformer oil aging sensor are another type of usage area for MTM sensors. Fuel adulteration is such a global problem especially in Asian countries where the governments applies strict polies to prevent oil adulterations which sometimes reach up to 30% [23]. Density, emission test and filter paper test methods have been implemented in sensing the fuel adulteration. These methods are laboratory based and the prices of the equipment used in these methods are high [24-25].

Measuring the dielectric properties of transformer oils used in power systems is commonly conducted. Measuring with transmission/reflection method has done for transformer oil before and after process in [26]. Transformer oil is basically the refined mineral oil which is extracted from crude oil by distillation. This oil is used as an insulator, therefore, its insulation and cooling properties are high. Having high purity and long life are also expected from transformer oils. In order to examine the characteristics of oil, complex and expensive chemical methods can be applied. Antennas designed by using microstrip structures can also be applied for transformer oil as in [27]. By varying the height of the transformer oil layer, the volume ratio between air and liquid can be changed as a function of this height. Due to the production and testing needs, this technique may not always applicable to sensor studies and it must be reconfigured when the material under test has been changed. Our method used in this study is similar to the method used in [27, 28]. Single side metamaterial is designed, simulated and tested for transformer oil. The base of these studies depends on adding particles by changing the resonance frequency.

This study has been conducted to reveal an alternative method for adulteration and transformer oil aging sensor with minimum disadvantages. In this study, we have developed a chiral MTM sensor based on square ring resonators which are placed on low loss Arlon DiClad 527 material which will be explained in the next section with details. Since waveguide boundaries present sensitive measurement with limited options, we have also developed a sensor layer which is based on a method initially used for measuring dielectric constant of materials in 2003 [28]. Variation in sensor layer's dielectric characteristics results in a resonance shift in reflectance of the proposed chiral metamaterial. Therefore, frequency shifts measured from reflectance pattern can be used for sensing physical and biological parameters of the samples placed in the sensor layer. By utilization of this sensor layer, we have succeeded practical, sensitive and fast measurements for transformer oil aging and fuel adulterations. Our study differs from the mentioned studies with the fact that it has a greater quality factor and shows wider application areas as microfluidic sensing of methanol, acetone and olive oil.

Organization of the study is as follows, design and materials along with the sensor layer is introduced in Section 2. In Section 3, numerical and experimental findings have been presented. The obtained results are discussed in Section 4.

II. THEORY, DESIGN AND NUMERICAL SETUP

In microwave characterization of the metamaterial based sensor applications, resonance cavity [29], proximity [30] and waveguide [31] methods are frequently used. When a material with known dielectric constant is placed into the sensor layer for characterization, the capacitance decreases or increases. In all three methods, when a material with given permittivity is placed into the sensor for characterization, a capacitor effect is created [20] which is directly related to the size of the sample holder. Due to the capacitive effects of a material placed in a sample holder, resonance frequency shifts to the upper or lower frequencies according to the material' complex permittivity values. Our proposal in this study is waveguide based since developed sample holder is complying with X band WR90 waveguide. When we compare the proposed structure with similar waveguide based studies as in [27,28], our proposed structure has a wider bandwidth and a greater quality factor which are important parameters for sensor applications since similar structures are compatible for only dielectric constant values varying between 1-3. When different materials such as methanol, acetone, petrol, diesel or transformer oil are considered, the resonance frequency is expected to shift lower or higher frequencies according to the material's complex permittivity values. In order to explain sensor usage of the proposed structure, we have initially measured the complex permittivity values of materials by using 85070E dielectric probe kit which is employed with the vector network analyzer. The samples were then placed into the sample holder and the reflection coefficients of the samples were measured. After having both reflection coefficient and complex permittivity values, we entered the obtained information about the materials and microfluidics into the electromagnetic simulation software to design the sensor structure. Fluid materials inside the sample holder are sensitive to the frequency due to its complex permittivity values. As the frequency increases, the effects of the material become more visible compared to the lower frequencies. For this reason, we have decided to work in X band which is between 8GHz and 12 GHz where the mentioned effects are more visible.

In this study, chiral shaped metamaterial that has nested split square resonators is placed on low loss Arlon DiClad 527 material having a dielectric constant of 2.5 and loss tangent of 0.0022. Nested square split rings have 135° angle difference in order to increase the mutual capacitance and inductance effects. As shown in Fig. 1 (b), back side resonators have different angles from the front side resonators. This design is especially chosen by simulation studies for maximum sensitivity. Resonators on back and front side are composed of copper that has a thickness of 0.035mm and conductivity of 5.8 x 10^6 S/m. Dimensions of the proposed structure is given in Fig. 1 (c). As briefly shown in Fig. 1 (d), the front and back side of the waveguide sample holder was closed with 25µm kapton film which was also added to simulation to simulate accurately as in experimental conditions.

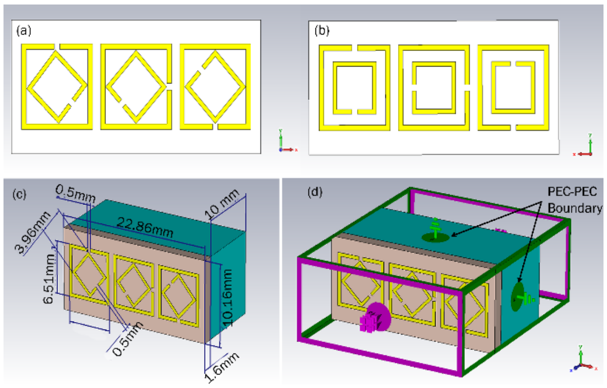

Fig. 1. Proposed structure: (a) front view, (b) back view, (c) dimensions of the structure, and (d) PEC-PEC boundary conditions.

Transformer oil and alcohol derivatives were placed in the sensor layer and outputs were read by a vector network analyzer. For this reason, all measurement system can be accepted as non-destructive and real time. Metamaterial sensor outputs are directly affected from the material's dielectric constant which is placed inside the sensor layer. For best sensitivity, sensor dimensions are optimized for X band operation. After the design phase, we manufactured the proposed structure by using LPKF Laser & Electronic AG, Promat E33 model Computerized Numerical Control (CNC) and printed circuit board (PCB) machine as presented in Fig. 2 (a). For sample placement and measurements, sample holder was produced by the same materials with WR90 waveguides in order to decrease physical effects during measurements. Manufactured sample holder seen in Fig. 2 (b) has a thickness of 10 mm and is placed between a WR90 waveguide and a corresponding adaptor as shown in Fig. 2 (d). Complex permittivity measurements in this study has been performed by employing 85070E dielectric probe kit as shown in Fig. 2 (c) after a complete calibration using pure water, air and a calibration kit associated with the probe. The complete measurement setup is given in Fig. 2 (d).

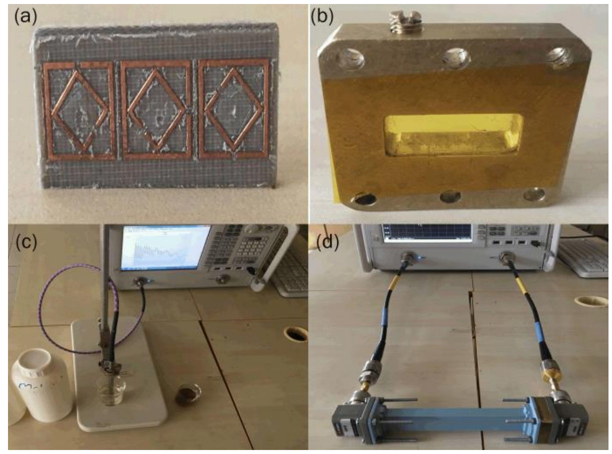

Fig. 2. (a) Manufactured CMS structure by using LPKF E-33 CNC machine (front side), (b) sample holder and kapton film which is used to prevent leakage from sample holder, (c) measurement of dielectric constant of new (left side) and used (right) side by using 85070E dielectric measurement kit, and (d) S11 reflection coefficient measurement picture.

The complex permittivity can have real and imaginary components, such that $\varepsilon=\varepsilon'-j\varepsilon''$. Thus, the loss tangent is defined as the ratio of the imaginary to real part of the complex permittivity ($\delta=\varepsilon''/\varepsilon'$). In this study, permittivity and loss tangent of the samples which are going to be tested in X- band, obtained from Agilent 85070E Dielectric probe kit. In order to prevent calibration and test errors, calibration process has been performed according the current state of art in X band.

Open-ended coaxial probe (OCP) method is currently one of the most popular techniques for measuring the complex dielectric permittivity of many materials. Non-destructive, broadband (RF and microwave ranges), and high-temperature measurements can be performed with this method using commercially available dielectric probe kits. Its well-developed theory makes it possible to obtain sufficiently accurate results for both medium-loss and high-loss media

S-parameters describe the relationship between the input and output ports and they can be used in the sensor applications of metamaterials [27-28]. In this study, we used S11 parameter also known as the return loss which refers to the reflection coefficient parameter (port 1 to port 1) with time gating experimentally measured by a Vector network analyzer (VNA). S_{11} parameter was utilized for validation of transformer oil fuel status and fuel adulteration sensing by using TE polarization mode which is the propagation mode where the electric field is normal (transverse) to the incident wave.

Our sensor is based on a waveguide design and it is suitable for materials with low dielectric constants about 1.8 to 2.6 in our case. The experimental studies were conducted by placing different materials with different dielectric constants according to its physical properties such as purity. Resonance frequency is measured by VNA and it was observed that this frequency shifts in terms of the dielectric constant of the material when it is placed into the sensing layer. After having a shift in the resonance frequency, we can comment about the purity or other physical properties of the sample under test. This procedures was performed for used and unused transformer oils, as well as in the gasoline and methanol purity measurements.

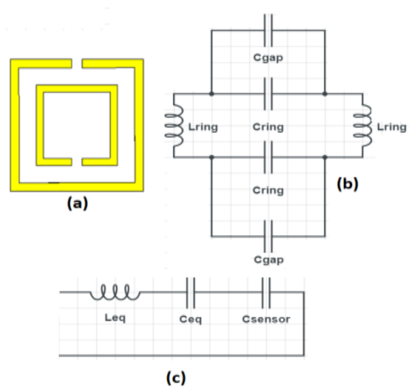

Fig. 3. Equivalent circuit diagram of the SRR.

The equivalent circuit model of the proposed sensor structure is drawn which can be seen in Fig. 3. The structure includes different passive elements labeled as Lring, Cring and Cgap. Lring represents the inductive effects of the resonator, Cring also known as capacitive effect occurs between two resonator layers and finally Cgap equals to the capacitive effect between the gaps. This equivalent circuit model is obtained based on SRR types of metamaterials [32]. In addition, the sensor layer which is placed at the back side of the structure creates capacitive effect on the structure. The final equivalent circuit diagram contains serially connected passive elements called as Leq, Ceq and Csensor and the final diagram is given in Fig. 3 (c):

$$\boldsymbol{C_{tot}}:\boldsymbol{C_0}+\boldsymbol{C_{eq}}+\boldsymbol{\varepsilon_{\mathrm{samp}}}\mathbf{c_{sens}}. \qquad (1)$$

$\boldsymbol{C_0}$ is the environmental capacitive effect which is formed due to the air and dielectric layer. In addition, Ceq is the total capacitive value of the resonator layer. Furthermore, $\boldsymbol{\varepsilon_{\mathrm{samp}}}\boldsymbol{C_{\mathrm{sens}}}$ is the capacitice effect of the sensor layer placed at the back side of the structure. That capacitive effect will change with the help of inserting different types of dielectric values ($\boldsymbol{\varepsilon' + \varepsilon''}$) of material. Therefore, the total capacitive effect will change leading to different resonant frequency values for the sensor layer. The corresponding resonant frequency can be expressed by:

$$f_0=1/(2\pi\sqrt{L_{tot}C_{tot}}). \qquad (2)$$

III. RESULTS AND DISCUSSION

A. Transformer oil sensing application

As shown in Fig. 1, sample holder is just behind the proposed structure and the material under test which is affecting the reflection coefficient of the system. First of all, the validation is realized with clear and dark transformer oil. In this work, all simulations and experimental tests have been performed in X-band between 8GHz and 12GHz which is compatible with WR-90 standard waveguide. As shown in Fig. 4, complex permittivity of the clear oil is higher than the dark transformer oil between 8-GHz and 12GHz. The results in the Fig. 3 show that, increasing the ratio of nanoparticles decreases the complex permittivity because of the oil saturation [27].

After obtaining the complex permittivity values of the industrial oil, these data were used in the simulation software to identify the mentioned oils in the computer environment. The simulation study was then performed and the obtained results were presented in Fig. 5 with the experimental results for comparison. When clear oil was placed in the setup, the resonance frequency is observed at 8.78 GHz. After determining the resonance point for the clear oil (unused), the sample was replaced with dark transformer oil (used). In this case, the resonance frequency decreased down to 8.71GHz dramatically as expected from the simulation results. This shift is directly related with the complex permittivity values of the samples placed in sample holder. Complex permittivity is directly proportional with capacitance which is inversely proportional with resonance frequency for this setup.

Reflection coefficients of these two oil samples have been simulated and tested by CST Microwave studio and Agilent PNA series network analyzer, respectively. 70MHz difference is observed during the simulation while testing the dark (used) and clear (unused) transformer oils. Measured and simulated results of the reflection coefficient are compatible with each other and the minimum calculated quality factor is greater than 290. This value is higher than that in similar metamaterial sensor studies in literature [33-35]. Although 70MHz for dark and clear transformer oil may look small, it still provides a significant margin to distinguish the samples easily when the vector network analyzer is employed. Bandwidth is important for sensitivity of the structure and this small bandwidth is also expected from the small differences observed in complex permittivity values of clear and dark transformer oils. As seen in Fig. 4, the dielectric constant values are 2.8 and 2.7, respectively while tangent loss values remain the same. Small mismatches between simulation and tests can be seen in Fig. 4, which were caused by the calibration and test errors of the system.

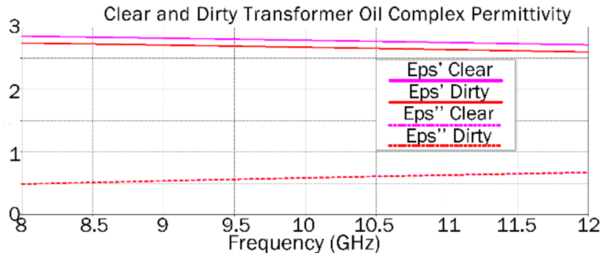

Fig. 4. Complex permittivity values of dark and clear transformer oil between 8 GHz – 12 GHz which is measured by open ended probe and 85070E dielectric measurement kit.

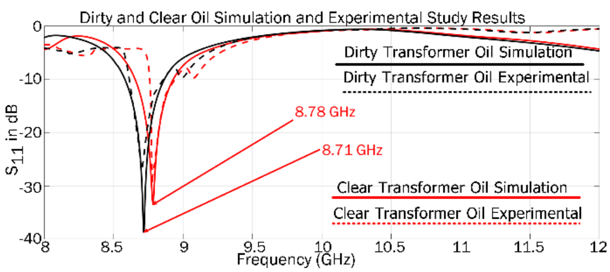

Fig. 5. Simulated and measured reflection coefficients of clear and dark transformer oil between 8GHz – 12 GHz.

In order to explain the operation principle of the proposed chiral metamaterial sensor, surface current distribution at the resonance frequency of 8.71 GHz which is belong to the used transformer oil was simulated and surface current distribution is plotted below. It is clearly understood from the Fig. 6 that the surface current generally concentrated on the resonators due to the strong magnetic fields. In addition, we can observe that parallel and anti-parallel surface current distributions take place on the resonator layers. While parallel current takes place due to the electric field, anti-parallel current occur because of the magnetic fields. This figure also explains the importance and behavior of the resonators at the resonant frequency.

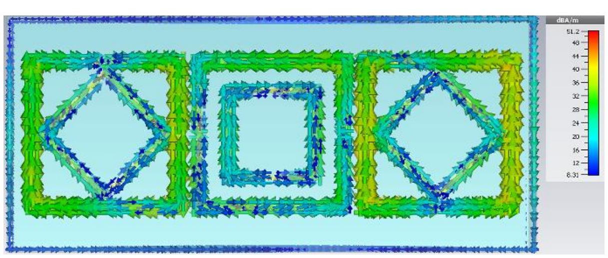

Fig. 6. Simulated surface current distribution at the resonance frequency of 8.71 GHz for used transformer oil.

B. Alcohol (microfluidic) sensing application

Another type of validation which was performed here is related with alcohols. Alcohols are particularly chosen since they are commonly used in chemical industry and to represent other microfluidics' validation. For this purpose, three different volume fractions of methanol – distilled water mixtures had been prepared. These are, pure methanol, 20% water with 80% methanol and 80% water with 20% methanol, respectively. For this setup, we have replaced the used and unused transformer oils with methanol – water mixtures to show the resonance frequency shifts. As previously performed, complex permittivity values of these samples have been measured by using 85070E dielectric measurement kit and network analyzer. Measurement results between 8GHz and 12GHz are presented in Fig. 7. Figure 7 shows a good example of Debye dielectric relaxation for methanol at 23°C with single relaxation time measured with an open-ended coaxial probe connected to a vector network analyzer. At lower frequencies, in a static region where the dipoles have time to follow the variations of the applied field, the dielectric constant of methanol mixtures which is prepared by using three different volume fractions of water and methanol reaches to maximum values. Similarly, dielectric constant values decrease in accordance with the formulas given in [36].

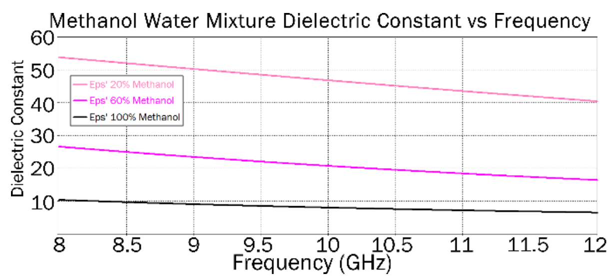

Fig. 7. Methanol & water mixture dielectric constant measurement results between 8 GHz – 12 GHz.

As seen clearly from the figure, while dielectric constant of pure methanol starts from 10, the others start from 27 and 55, respectively. Their values decrease as the frequency increases. After having complex permittivity values, the overall structure has been simulated by entering the experimentally obtained dielectric constant values to the sample holder in the computer environment. In order to validate the simulation results, we have also prepared samples for methanol and measured their reflection coefficients. The simulated and tested reflection coefficient parameters are presented in Fig. 8. As it is seen from the figure, 210MHz bandwidth is observed between pure methanol and 20% methanol. Resonance frequency for 100% methanol was obtained at 9.17 GHz, this value increased to 9.26 GHz when 20% percent distilled water added into the methanol solution. When volume fraction of water increased to 80%, resonance frequency increased to 9.38 GHz. One of the important features of sensors is linearity and it is clearly seen from the figure that the results are linear both in simulation and the experimental testing.

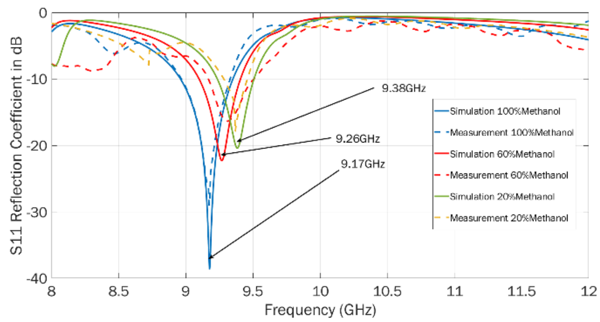

Fig. 8. S_{11} reflection coefficient measurement and simulation comparison between 8 GHz – 12 GHz for 100% volume fraction of Methanol, 60% volume fraction of methanol and 20% volume fraction of methanol with water mixture.

C. Olive oil adulteration example

Another example for the usage of the proposed metamaterial sensor is olive oil adulteration. Since the production of olive oil decreases and controversially the demand on it increases, some manufacturers mix olive oil with corn, palm, sunflower seed or other oils. In this part, we have prepared two samples; which are olive oil and corn oil. As the first step which is similar to the procedure mentioned before, we performed a complex permittivity measurement of these samples, after that we simulated and tested the reflection coefficient by using our proposed structure. As it is seen from Fig. 9, complex permittivity values of the olive oil and corn oil are very similar between 8GHz and 12GHz which is measured by calibrated 85070E dielectric probe kit. As it is seen from Fig. 7, Reel part of the complex permittivity of 100% olive oil' dielectric constant starts from 2.78 while corn oil starts from 2.6. After the experimental measurement of dielectric constant, a set of simulation and test results related to different oil samples are plotted in Fig. 10. Simulated S_{11} parameter when sample holder is filled with corn oil has the resonance frequency at 8.61 GHz while olive oil resonance frequency is observed at 8.56 GHz. Tested resonance frequencies for olive and corn oil samples are similar to the simulated ones. Small errors were observed during testing because of the laboratory environment, testing cable losses and calibration errors of the network analyzer. Compatible results with alcohol and transformer oil validations have also been observed. Losses in the simulation and testing are caused from loss tangent of the oils. Although 50MHz difference may seem to be small value for sensors, it can be sensed easily by a calibrated vector network analyzer.

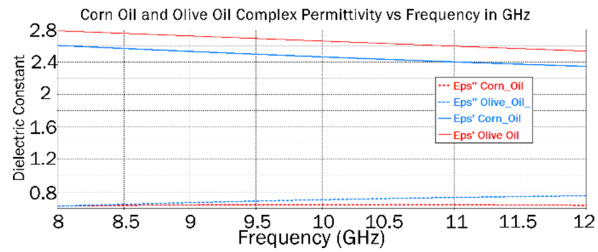

Fig. 9. Corn oil and olive oil complex permittivity measurements between 8GHz – 12 GHz by using calibrated 85070E dielectric probe kit.

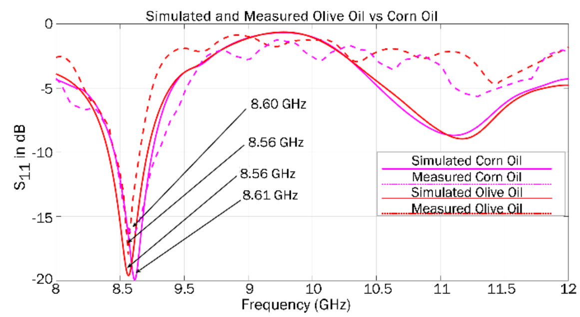

Fig. 10. S_{11} reflection coefficient measurement and simulation comparison of pure corn oil and olive oil between 8GHz – 12 GHz.

D. Simulation of reflection coefficient for multipurpose sensing

In this section, we have simulated the reflection coefficient parameters of the proposed metamaterial sensor for different fluid sensing applications. In order to show application examples of the proposed structure, we have measured the complex permittivity values of acetone, clear oil (unused transformer oil), dark oil (used transformer oil) and methanol. Obtained values are given in Table 1. In order to show the wide range of sensor application of the proposed structure, we have simulated the reflection coefficient when the sample holder was filled with these materials. Simulated reflection coefficient plot is presented in Fig. 11. According to the figure, when dielectric constant increased from 2.73 to 24, resonance frequencies of the reflection coefficients are increased from 8.71 GHz to 9.27 GHz which means that total bandwidth is 560MHz which corresponds to the dielectric constant changes.

Table 1: Dielectric constant values of some of the fluid measured between 8 GHz – 12 GHz by using 85070E dielectric probe kit

Material	Dielectric Constant
Acetone	24
Clear Oil	2.85
Dark Oil	2.73
Methanol	10.40

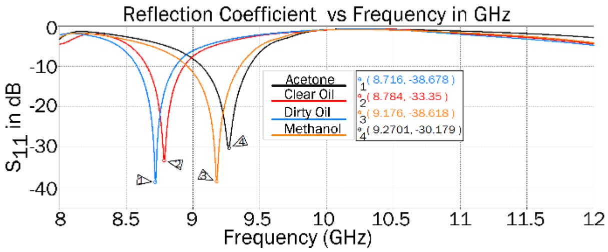

Fig. 11. Simulated reflection coefficient S_{11} parameter of the proposed structure when sample holder is filled with acetone, clear oil, dark oil and methanol between 8 GHz–12 GHz.

IV. CONCLUSION

A novel shaped metamaterial based sensor composed of traditional split square rings have been proposed to operate in X-band for sensing transformer oils and other fluid materials as methanol purity and olive oil adulteration. One of the important part of the proposed study is to have compatible operation for materials whose dielectric constants varying from 2 to 24 with high quality factor when it is compared with similar studies. Simulation studies have been validated with experimental ones. Generally, compatible results have been observed between them. Dielectric constant values are directly affecting the resonance frequency as well as the quality factor. If dielectric constants of the materials under test are close to each other, the resonance frequency difference between them would also be close to each other which can be counted as a weak part of this study. Due to the wide range of dielectric constant response, we believe that the proposed structure can be adapted to other microfluidic sensor applications.

ACKNOWLEDGMENT

We would like to thank the Scientific and Technological Research Council of Turkey (117M855) for the financial support.

REFERENCES

[1] M. Karaaslan and M. Bakir, “Chiral metamaterial based multifunctional sensor applications,” *Progress In Electromagnetics Research*, vol. 149, pp. 55-67, 2014.

[2] L. Changjun and T. Fan, “An SIW resonator sensor for liquid permittivity measurements at C band,” *IEEE Microwave Wirel. Compon. Lett.*, vol. 25, no. 11, pp. 751-753, 2015.

[3] M. Bakir, M. Karaaslan, F. Dincer, O. Akgol, and C. Sabah, “Electromagnetic energy harvesting and density sensor application based on perfect metamaterial absorber,” *International Journal of Modern Physics B*, vol. 30, no. 20, p. 1650133, 2016.

[4] A. Ebrahimi, W. Withayachumnankul, S. Al-Sarawi, and D. Abbott, “High-sensitivity metamaterial-inspired sensor for microfluidic dielectric characterization,” *IEEE Sensors J.*, vol. 14, no. 5, pp. 1345-1351, 2014.

[5] A. Salim, S. H. Kim, J. Y. Park, and S. Lim, “Microfluidic biosensor based on microwave substrate-integrated waveguide cavity resonator,” *Journal of Sensors*, 1324145, pp. 1-13, 2018.

[6] J. F. Sadat, K. Fatemeh, and A. S. Javad, “Nondestructive aging of transformer oil using electromagnetic waves,” *Elect. Power Distribut. Net. Conf. (EPDC), 2015 20th Conf. IEEE*, pp. 277-9, 2015.

[7] S. Guenneau, C. Amra, and D. Veynante, “Transformation thermodynamics: Cloaking and concentrating heat flux,” *Optics Express*, vol. 20, no. 7, pp. 8207-8218, 2012.

[8] D. Shrekenhamer, W. Chen, and W. J. Padilla, “Liquid crystal tunable metamaterial absorber,” *Phys. Rev. Lett.*, vol 110, 177403, 2013.

[9] M. Mrnka, P. Vasina, M. Kufa, V. Hebelka, and Z. Raida, “The RF energy harvesting antennas operating in commercially deployed frequency bands: A comparative study,” *International Journal of Antennas and Propagation*, vol. 2016, Article ID 7379624, 11 pages, 2016. doi:10.1155/2016/7379624.

[10] T. Almoneef and O. M. Ramahi, “A 3-dimensional stacked metamaterial arrays for electromagnetic energy harvesting,” *Progress In Electromagnetics Research*, vol. 146, pp. 109-115, 2014.

[11] M. Schueler, C. Mandel, M. Puentes, and R. Jakoby, “Metamaterial inspired microwave sensors,” *IEEE Microwave Magazine*, vol. 13, no. 2, pp. 57-68, 2012.

[12] A. Vora, J. Gwamuri, N. Pala, A. Kulkarni, J. M. Pearce, and Ö. D. Güney, “Exchanging ohmic losses in metamaterial absorbers with useful optical absorption for photovoltaics,” *Sci. Rep.*, vol 4, p. 4901 2014.

[13] M. Bakır, M. Karaaslan, F. Dincer, K. Delihacioglu, and C. Sabah, “Tunable perfect metamaterial absorber and sensor applications,” *J. Mater. Sci. Mater. Electron.*, vol. 27, pp. 12091-12099, 2016.

[14] M. Bakır, M. Karaaslan, O. Altıntaş, M. Bagmancı, V. Akdogan, and F. Temurtaş, “Tunable energy harvesting on UHF bands especially for GSM frequencies,” *International Journal of Microwave and Wireless Technologies*, vol. 10, pp. 67-76, 2018.

[15] G. Galindo-Romera, F. J. Herraiz-Martínez, M. Gil, J. J. Martínez-Martínez, and D. Segovia-Vargas, “Submersible printed split-ring resonator-based sensor for thin-film detection and permittivity characterization,” *IEEE Sens. J.*, vol. 16, pp. 3587-3596, 2016.

[16] N. Wiwatcharagoses, K. Y. Park, J. Hejase, L. Williamson, and P. Chahal, “Microwave artificially

structured periodic media microfluidic sensor," *in Proc. IEEE 61st Electronic Components and Technology Conference (ECTC)*, pp. 1889-1893, 2011.

[17] A. A. Abduljabar, D. J. Rowe, A. Porch, and D. A. Barrow, "Novel microwave microfluidic sensor using a microstrip split-ring resonator," *TMTT*, pp. 679-688, 2014.

[18] W. Withayachumnankul, K. Jaruwongrungsee, A. Tuantranont, C. Fumeaux, and D. Abbott, "Metamaterial-based microfluidic sensor for dielectric characterization," *Sensors and Actuators A: Physical*, vol. 189, pp. 233-237, 2013.

[19] M. Bakır, "Electromagnetic-based microfluidic sensor applications," *J. Electrochem. Soc*., vol. 164, no. 9, pp. B488-B494, 2017.

[20] A. Ebrahimi, W. Withayachumnankul, S. Al-Sarawi, and D. Abbott, "High-sensitivity metamaterial-inspired sensor for microfluidic dielectric characterization," *IEEE Sensors J*., vol. 14, no. 5, pp. 1345-1351, 2014.

[21] M. Yoo, H. K. Kim, and S. Lim, "Electromagnetic-based ethanol chemical sensor using metamaterial absorber," *Sensors and Actuators B: Chemical*, vol. 222, pp. 173-180, 2016.

[22] C. A. Agostini, "Differential fuel taxes and their effects on automobile demand," *Cepal Rev*., vol. 102, pp. 101-111, 2010.

[23] V. J. Felix, P. A. Udaykiran, and K. Ganesan, "Fuel adulteration detection system," *Indian J. Sci. Technol*., vol. 8, no. S2, pp. 90-95, 2015.

[24] S. Kher, S. Chaubey, J. Kishore, and S. M. Oak, "Detection of fuel adulteration with high sensitivity using turnaround point long period fiber gratings in b/ge doped fibers," *IEEE Sensors J*., vol. 13, no. 11, pp. 4482-4486, 2013.

[25] S. Wang, L. Zhu, and W. Wu, "A novel frequency-reconfigurable patch antenna using low-loss transformer oil," in *IEEE Transactions on Antennas and Propagation*, vol. 65, no. 12, pp. 7316-7321, 2017.

[26] F. S. Jafari, F. Kazemi, and A. S. Javad, "Non-destructive aging of transformer oil using electromagnetic waves," *2015 20th Conference on Electrical Power Distribution Networks Conference (EPDC)*, Zahedan, pp. 277-279, 2015.

[27] F. S. Jafari and A. S. Javad, "Frequency-selective surface to determine permittivity of industrial oil and effect of nanoparticle addition in X-band," *J. Electron. Mater*., vol. 47, pp. 1397-1404, 2018.

[28] Y. Wang and M. N. Afsar, "Measurement of complex permittivity of liquids using waveguide techniques," *Progr. Elect. Res*., vol. 42, pp. 131-142, 2003.

[29] K. Bhattarai, S. Silva, K. Song, A. Urbas, S. Lee, Z. Ku, and J. Zhou, "Metamaterial perfect absorber analyzed by a meta-cavity model consisting of multilayer metasurfaces," *Scientific Reports*, vol. 7, pp. 10569, 2017.

[30] S. Qiu, Y. Huang, X. He, Z. Sun, P. Liu, and C. A. Liu, "Dual-mode proximity sensor with integrated capacitive and temperature sensing units," *Measurement Science and Technology*, vol. 26, pp. 105101, 2015.

[31] F. S. Jafari and A. S. Javad, "Reconfigurable microwave SIW sensor based on PBG structure for high accuracy permittivity characterization of industrial liquids," *Sensors and Actuators A: Physical*, vol. 283, pp. 386-395, 2018.

[32] S. Naoui, L. Latrach, and A. Gharsallah, "Equivalent circuit model of double split ring resonators," *International Journal of Microwave and Optical Technology*, vol. 11, no. 1, pp. 1-6, 2016.

[33] M. Bakır, M. Karaaslan, E. Unal, O. Akgol, and C. Sabah, "Microwave metamaterial absorber for sensing applications," *Opto-Electronics Review*, vol. 25, p. 318, 2017.

[34] O. Altıntaş, M. Aksoy, O. Akgol, E. Unal, M. Karaaslan, and C. Sabah, "Fluid, strain and rotation sensing applications by using metamaterial based sensor," *J. Electrochem. Soc*., vol. 164, no. 1), pp. B567-B573, 2017.

[35] A. Salim and S. Lim, "Review of recent metamaterial microfluidic sensors," *Sensors*, vol. 18, pp. 232, 2018.

[36] P. M. Meaney, A. P. Gregory, J. Seppälä, and T. Lahtinen, "Open-ended coaxial dielectric probe effective penetration depth determination," in *IEEE Transactions on Microwave Theory and Techniques*, vol. 64, no. 3, pp. 915-923, 2016.